JOURNAL OF GUIDANCE, CONTROL, AND DYNAMICS
Vol. 19, No. 2, March–April 1996

Inverse and Optimal Control for Precision Aerobatic Maneuvers

K. Y. Lou*
Defence Science Organization, Singapore 118230, Singapore
and
A. E. Bryson†
Stanford University, Stanford, California 94305

Control input histories are determined for flying precision three-dimensional aerobatic maneuvers using inverse-control and optimization methods. A point-mass model is used with three controls, angle of attack, bank angle, and thrust. Bounds are placed on normal load factor, thrust, and angle of attack. By choosing cylindrical coordinates for the position vector and spherical coordinates for the velocity vector, simple inverse solutions are found for precision aerobatic maneuvers. Requiring constant radius and constant helix angle produces nonlinear feedback laws for angle of attack and bank angle. Numerical results are presented for an F4H aircraft performing barrel rolls.

Introduction

AEROBATIC maneuvers are the ultimate art of flying. They require keen reflexes in the pilot and close coordination of the various controls. The aerobatic aircraft must be structurally sound, have a large wind area, and have an engine that is powerful relative to its weight. The American Pitts special, with a composite structure and a modified engine, achieves a thrust/weight ratio well above 1. Most fighters can also perform such maneuvers because of their powerful engines (e.g., the maximum thrust/weight ratio of an F-16 ranges between 1.0 and 1.4). Aerobatic maneuvers are an integral part of a fighter pilot's tactics in aerial combat and help him to recover from unexpected flight conditions such as spins.[1] For example, a high-g barrel roll is often effective against an attacker closing from astern. Immelman or split-S maneuvers are standard methods of disengaging from combat.[2]

In conventional flight control design, the aircraft dynamics are assumed linear and time invariant about some nominal equilibrium flight trajectory. These assumptions are not valid in aerobatic maneuvers because they generally involve large changes in aircraft altitude and attitude. This study develops a systematic approach to determine the control inputs for specified aerobatic maneuvers. The approach uses inverse and optimal control methods to generate feedforward control histories. A unified approach for analyzing precision aerobatic maneuvers is presented by specifying the flight path as either a horizontal or a vertical helix. These specifications are then used in inverse analysis to generate the controls. If the resulting controls are not feasible or if terminal conditions are not met, optimal control methods are used to satisfy the constraints while minimizing the deviations from the ideal aerobatic maneuver.

Uehara et al.[3] considered minimum time loop maneuvers using a point-mass model. They showed that the controls are mainly on the control boundaries (i.e., bang–bang). A similar study by Shinar et al.[4] used an energy state model. They showed that by using this reduced-order model, the solution can be expressed in a feedback form. In recent years, inverse control methods have been used to analyze large-amplitude aircraft motions. Kato and Sugiura[5] presented an aileron roll maneuver as an example of inverse analysis of aircraft motion. In their example, however, the inverse control magnitudes are not feasible. Hess et al.[6] found the inverse controls for the same maneuver using an inverse simulation technique. A rigid-body model was used in both cases. In another paper by Kato[7] a barrel roll maneuver was analyzed using an attitude projection method. He specifies the maneuver from a pilot's point of view, i.e., in terms of aircraft body attitudes. Sentoh[8] considered the aileron roll maneuver example of Kato and Sugiura[5] using an optimal control method with the inverse control solution as an initial guess; this resulted in a maneuver with feasible control inputs and only slight deviations of the center of mass from the desired straight line path.

Received June 7, 1995; presented as Paper 95-3328 at the AIAA Guidance, Navigation, and Control Conference, Baltimore, MD, Aug. 7–10, 1995; revision received Aug. 11, 1995; accepted for publication Oct. 27, 1995.

*Project Engineer, 20, Science Park Drive. Member AIAA.
†Pigott Professor of Engineering Emeritus, Department of Aeronautics and Astronautics. Honorary Fellow AIAA.

Equations of Motion

In this section, we present a derivation of equations of motion using clock/cone/bank angles. This wind axis coordinate system is useful for analyzing loops, barrel rolls, Immelmans, and split-S maneuvers. The velocity vector relative to inertial space is described by its magnitude V, the clock angle γ_c, and the cone angle χ_c. The direction of the lift force is described by a rotation about the velocity vector through the bank angle μ_c (see Fig. 1). Whereas velocity is a vector, when the direction of the lift force is added, the three angles $(\gamma_c, \chi_c, \mu_c)$ are Euler angles of the wind axes, and so the order of rotations is important.

The components of a vector in wind axes $x^{(w)}$ given its components in inertial axes $x^{(I)}$ are given by

$$x^{(w)} = T^1_{\mu_c} T^3_{\chi_c} T^1_{-\gamma_c} x^{(I)} \tag{1}$$

where T^i_α indicates a two-dimensional rotation about the i axis through an angle α.

The transformation of vector components to body axes from wind axes is made by two more rotations, through the angle of sideslip β, and the angle of attack α and is given by

$$x^{(b)} = T^2_\alpha T^3_\beta x^{(w)} \tag{2}$$

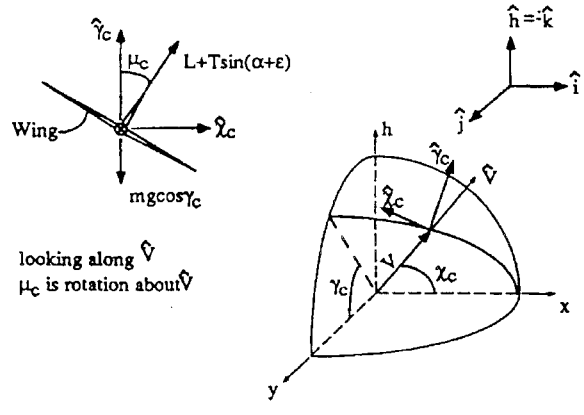

Fig. 1 Velocity vector and clock/cone/bank angles.

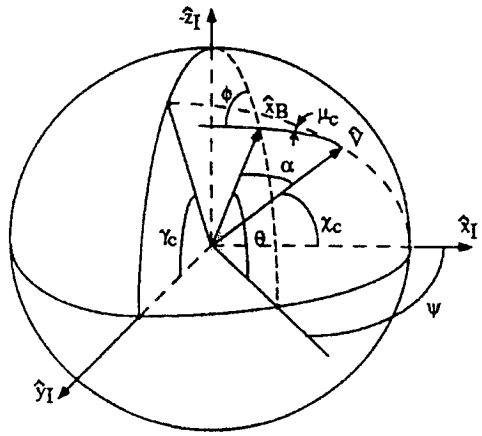

Fig. 2 Relationship of body and wind axes (χ_c, γ_c, μ_c) to inertial axes for $\beta = 0$: $\hat{x}_B$ = direction body x axis and $\hat{V}$ = direction velocity of c.m.

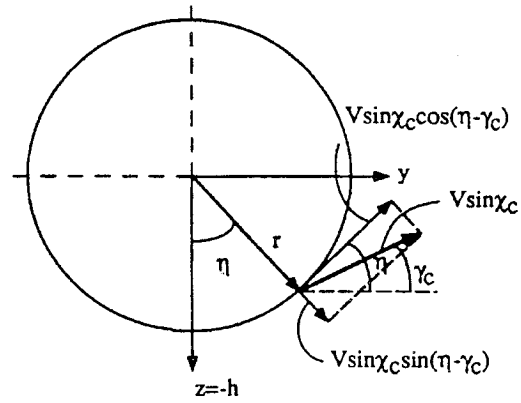

Fig. 3 Horizontal cylindrical position coordinates.

The body axes are located with respect to inertial axes by three Euler angles. The NASA standard Euler angles are ψ, θ, and ϕ, which are called yaw, pitch, and roll angles. The components of a vector in body axes given its components in inertial axes are

$$x^{(b)} = T_\phi^1 T_\theta^2 T_\psi^3 x^{(I)} \tag{3}$$

Equations (1–3) permit us to find the relationship between the wind-axis Euler angles (χ_c, γ_c, and μ_c) and the body-axis Euler angles (ψ, θ, and ϕ) given β and α. Equating Eq. (2) to Eq. (3) using Eq. (1) gives

$$T_\phi^1 T_\theta^2 T_\psi^3 = T_\alpha^2 T_\beta^3 T_{\mu_c}^1 T_{\chi_c}^3 T_{-\gamma_c}^1 \tag{4}$$

Equating terms gives the desired relations. For $\beta = 0$ (see Fig. 2),

$$-\sin\theta = -\cos\alpha \sin\chi_c \sin\gamma_c - \sin\alpha(\cos\mu_c \cos\gamma_c + \sin\mu_c \cos\chi_c \sin\gamma_c) \tag{5}$$

$$\tan\phi = \frac{\sin\mu_c \cos\gamma_c - \cos\mu_c \cos\chi_c \sin\gamma_c}{-\sin\alpha \sin\chi_c \sin\chi_c + \cos\alpha(\cos\mu_c \cos\gamma_c + \sin\mu_c \cos\chi_c \sin\gamma_c)} \tag{6}$$

$$\tan\psi = \frac{\cos\alpha \cos\gamma_c \sin\chi_c - \sin\alpha(\cos\mu_c \sin\gamma_c - \sin\mu_c \cos\chi_c \cos\gamma_c)}{\cos\alpha \cos\chi_c - \sin\alpha \sin\mu_c \sin\chi_c} \tag{7}$$

Kinematic Equations

We define the position of the center of mass by x, y, and h, where h is altitude and x and y are orthogonal horizontal position coordinates. It follows from Fig. 1 that

$$\dot{x} = V \cos\chi_c \tag{8}$$

$$\dot{y} = V \sin\chi_c \cos\gamma_c \tag{9}$$

$$\dot{h} = V \sin\chi_c \sin\gamma_c \tag{10}$$

For maneuvers like loops and barrel rolls horizontal cylindrical position coordinates (r, η, x) are useful (see Fig. 3), where

$$\dot{r} = V \sin\chi_c \sin(\eta - \gamma_c) \tag{11}$$

$$r\dot{\eta} = V \sin\chi_c \cos(\eta - \gamma_c) \tag{12}$$

$$\dot{x} = V \cos\chi_c \tag{13}$$

Dynamic Equations

The forces acting on the vehicle are thrust T, lift L, drag D, and gravitational force mg. The components of gravitational force in these wind axes with $\mu_c = 0$ are given by

$$g^{(w)} = T_{\chi_c}^3 T_{-\gamma_c}^1 g^{(I)} \tag{14}$$

Using the NASA standard coordinates (1 and 2 axes horizontal, 3 axis down) means that $g^{(I)} = g[0 \quad 0 \quad 1]^T$, and using this with Eq. (14) gives

$$g^{(w)} = g \begin{bmatrix} -\sin\gamma_c \sin\chi_c \\ -\sin\gamma_c \cos\chi_c \\ \cos\gamma_c \end{bmatrix}^T \tag{15}$$

The equations of motion in clock–cone–bank angle wind axis components are

$$m\dot{V} = T\cos(\alpha + \varepsilon) - D - mg \sin\chi_c \sin\gamma_c \tag{16}$$

$$mV \sin\chi_c \dot{\gamma}_c = [L + T\sin(\alpha + \varepsilon)]\cos\mu_c - mg\cos\gamma_c \tag{17}$$

$$mV\dot{\chi}_c = [L + T\sin(\alpha + \varepsilon)]\sin\mu_c - mg\cos\chi_c \sin\gamma_c \tag{18}$$

Equations (11–13) and (16–18) are the equations of motion for the analysis in the following sections. The three controls are angle of attack α, bank angle μ_c, and thrust T.

Inverse and Optimal Control

Here we present the approach of finding control inputs for loop/barrel roll maneuvers using inverse and optimal methods. A barrel roll maneuver involves a flight path about an imaginary cylinder (a barrel) with its axis parallel to the ground. The pilot selects a reference point on the horizon and makes the aircraft longitudinal axis describe a circle about that point.[1] It is a coordinated climbing and turning maneuver.

In a precision loop or barrel roll, an aircraft moves along a horizontal helix, where the radius r and the helix angle χ_c are both constant. This implies that $\dot{r} = \dot{\chi}_c = 0$. Note that the ranges of χ_c are $0 < \chi_c \leq \pi/2$. When $\chi_c = \pi/2$, it is a loop, and when $\chi_c \to 0$, the maneuver approaches that of an aileron roll. Using Eqs. (11), (12), and (18) we can determine the required bank angle μ_c and the normal force $N = L + T\sin(\alpha + \varepsilon)$ as nonlinear feedbacks on V and γ_c:

$$\tan\mu_c = \frac{\cos\chi_c \sin\gamma_c}{\cos\gamma_c + V^2 \sin^2\chi_c / gr} \tag{19}$$

$$N = mg\left[(\cos\chi_c \sin\gamma_c)^2 + \left(\cos\gamma_c + V^2 \sin^2\chi_c / gr\right)^2\right]^{\frac{1}{2}} \tag{20}$$

This reduces the equations of motion of interest to two, namely, Eqs. (16) and (17), since Eq. (13) does not involve any control.

Because the lift force is function of (V, h, α) [see Eq. (36)], α can be determined given (N, T, V, h). The only remaining control is the thrust T. By using γ_c as the independent variable, there is only one equation of motion for $V(\gamma_c)$. Dividing Eq. (16) by Eq. (17) gives

$$\frac{dV}{d\gamma_c} = \frac{T\cos(\alpha+\varepsilon) - D - mg\sin\chi_c \sin\gamma_c}{V\sin\chi_c/r} \tag{21}$$

The time histories can be obtained using Eq. (12) and the condition that $\eta = \gamma_c$:

$$\frac{dt}{d\gamma_c} = \frac{r}{V\sin\chi_c} \tag{22}$$

The block diagram in Fig. 4 shows the case where T is specified. The outputs are the position of the center of mass and the attitude of the aircraft. If the inverse solution does not satisfy the constraints on the controls, the normal load factor, or the terminal conditions, optimal control methods are used to modify the inverse solution. We are interested in the following optimal control problem:

$$\min f \tag{23}$$

where f is the performance index, subject to the equations of motion (21) and (22), the initial and terminal conditions

$$V(0) = V(t_f) = V_0 \tag{24}$$

where t_f is the final time, and the control constraints

$$|\alpha| \le \alpha_{\max}, \qquad |N| \le N_{\max}, \qquad 0 \le T \le T_{\max} \tag{25}$$

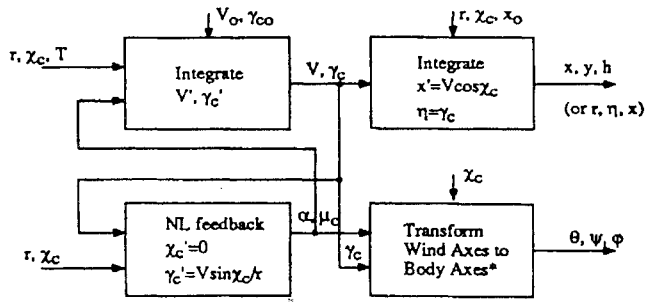

Fig. 4 Block diagram representation of inverse control for loop/barrel roll.

The optimal control problem is formulated as a nonlinear programming problem using Seywald's differential inclusion method.[9] For loop/barrel roll maneuvers, let the parameter vector be the velocity at n time points and the radius r,

$$k = [V(\gamma_c)_i, \ldots, V(\gamma_c)_n\, r] \tag{26}$$

where n is the number of discretization intervals. From the initial guess of $V(\gamma_c)_i, i = 1, \ldots, n-1$, and r determine $dt/d\gamma_c$, $dh/d\gamma_c$, and hence t_i, h_i using the discrete equations of motion

$$t_{i+1} = t_i + \frac{r}{\bar{V}\sin\chi_c}\, d\gamma_c \tag{27}$$

$$h_{i+1} = h_i + r\sin\gamma_c\, d\gamma_c \tag{28}$$

where $d\gamma_c = n/2\pi$, $\bar{(\,)} = [(\,)_{i+1} + (\,)_i]/2$, and $i = 1$ corresponds to initial conditions. To obtain the parameterized controls, compute $dV/d\gamma_c$ by numerically differencing the parameter vector $V_i, i = 1, \ldots, n-1$. Then define a_1 and a_2 as

$$a_1 = \sin\bar{\gamma}_c \cos\chi_c \tag{29}$$

$$a_2 = \cos\bar{\gamma}_c + \frac{(\bar{V}\sin\chi_c)^2}{gr} \tag{30}$$

The bank angle and normal load factor are then given by

$$\mu_c = \tan^{-1}(a_1/a_2) \tag{31}$$

$$N = mg\sqrt{a_1^2 + a_2^2} \tag{32}$$

The angle of attack and thrust are computed using a Newton–Raphson method from the following nonlinear equations:

$$\frac{dV}{d\gamma_c} - \frac{T\cos(\alpha+\varepsilon) + D + mg\sin\chi_c\sin\bar{\gamma}_c}{\bar{V}\sin\chi_c/r} = 0 \tag{33}$$

$$N - T\sin(\alpha+\varepsilon) - L = 0 \tag{34}$$

where

$$D = \tfrac{1}{2}\rho(h)C_D(M,\alpha)\bar{V}^2 \tag{35}$$

$$L = \tfrac{1}{2}\rho(h)C_L(M,\alpha)\bar{V}^2 \tag{36}$$

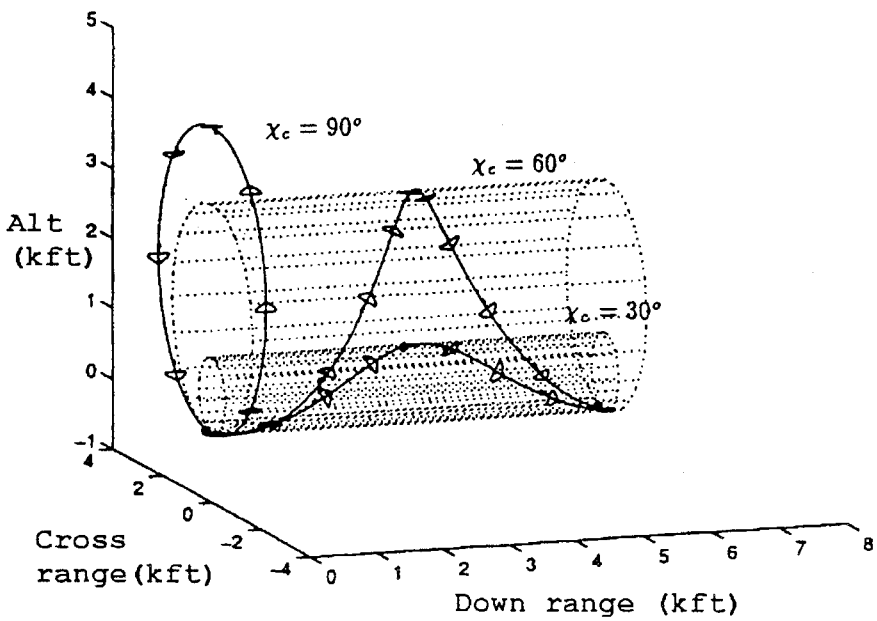

Fig. 5 Minimum radius loop/barrel rolls at sea level.

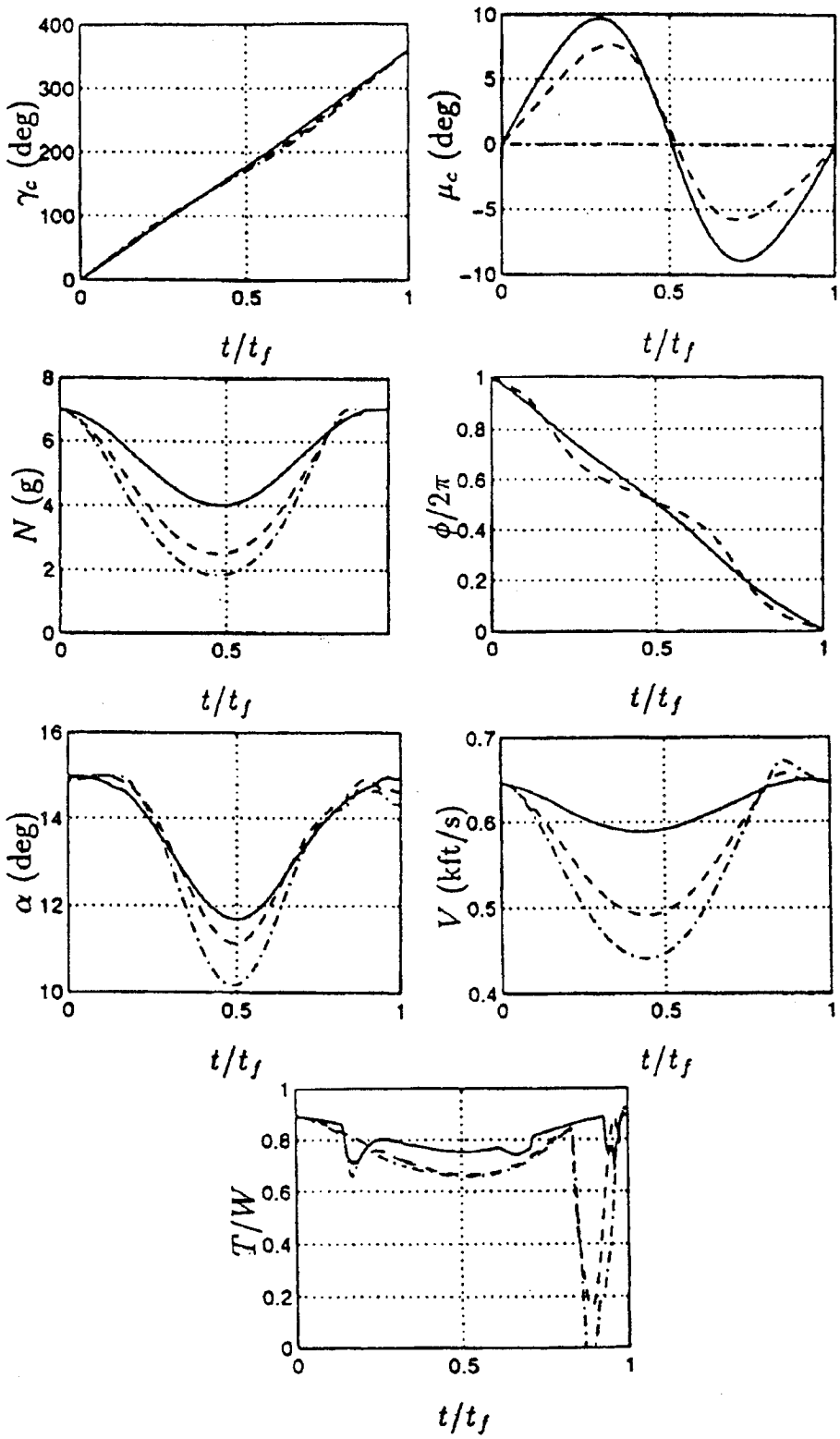

Fig. 6 State and control time histories for minimum radius loop/barrel rolls at sea level with V_0 open: ——, χ_c = 30 deg; - - -, χ_c = 60 deg; and ·····, χ_c = 90 deg.

There are no terminal constraints for a loop/barrel roll maneuver. The bounds on the controls and the load factor are inequality constraints

$$\alpha_i - \alpha_{\max} \leq 0 \tag{37}$$

$$N_i - N_{\max} \leq 0 \tag{38}$$

$$T_i - T_{\max} \leq 0, \qquad -T_i \leq 0 \tag{39}$$

for $i = 1, \ldots, n$. The performance index for a minimum radius loop/barrel roll is

$$f = r \tag{40}$$

The constrained parameter optimization problem can be solved readily using the MATLAB function constr.[10] The initial guess of the parameter vector k comes from the inverse control solution with constant thrust.

Numerical Results

In this section, we present numerical examples of loops and barrel rolls using an F4H aircraft model with constant weight $W = 35$ klb

and $\varepsilon = 0$. The aerodynamic and maximum thrust characteristics for the F4H (see the Appendix) are

$$C_L = C_{L_\alpha}\alpha \tag{41}$$

$$C_D = C_{D_0} + \bar{\kappa}C_L^2 \tag{42}$$

$$T_{\max} = [1,\ M,\ M^2,\ M^3,\ M^4]\, Q\, [1,\ h,\ h^2,\ h^3,\ h^4]^T \tag{43}$$

where C_{L_α}, C_{D_0}, and $\bar{\kappa}$ are functions of Mach number; Q is a 4×4 matrix of coefficients used to approximate the maximum thrust data as polynomials in Mach number M and altitude h. The problem here is to find the control histories [i.e., $\alpha(t)$, $T(t)$, $\mu_c(t)$] of a precision loop/barrel roll maneuver to minimize the radius subject to the following constraints:

$$\alpha_{\max} = 15\,\text{deg} \tag{44}$$

$$N_{\max} = 7\,g \tag{45}$$

Table 1 Summary of barrel roll/loop maneuvers for F4H

$V(0)$, kft/s	$\chi_c(0)$, deg	r, kft	t_f, s	n
0.65	30	0.54	11.0	150
0.65	60	1.63	20.6	150
0.65	90	2.18	24.8	150

All maneuvers begin at horizontal flight at sea level. The initial velocity is a parameter to be optimized. All maneuvers end with final velocity equal to the initial velocity.

Figures 5 and 6 show the trajectories and the state and control histories for the maneuvers. Table 1 summarizes the results for three different values of cone angle. From the results, the optimal entry velocity $V(0)$ for all cases turned out to be the same, namely, 0.65 kft/s. The optimal angle-of-attack history begins and ends at its maximum values. This is to provide the centripetal force for the maneuvers. The optimal thrust levels stay at $T_{\max}$ except for the loop at $\chi_c = 90$ deg, where T switches between $T = 0$ and $T_{\max}$ toward the end of the maneuver.

Conclusion

By choosing an appropriate dynamic model and coordinate system, the inverse control problem for aerobatic maneuvers is greatly simplified. The mass-point model is found to be adequate for the maneuvers considered. For loop/barrel roll maneuvers, cylindrical coordinates for the position vector and spherical coordinates for the velocity vector were found to simplify the inverse solution. Using these coordinate systems and specifying aerobatic maneuvers as motions along horizontal or vertical helices result in nonlinear feedback laws for two of the three controls. The nonlinear feedback laws reduce the number of controls to one.

If the inverse control solution does not satisfy constraints on controls, normal load factor, or terminal conditions, then a solution

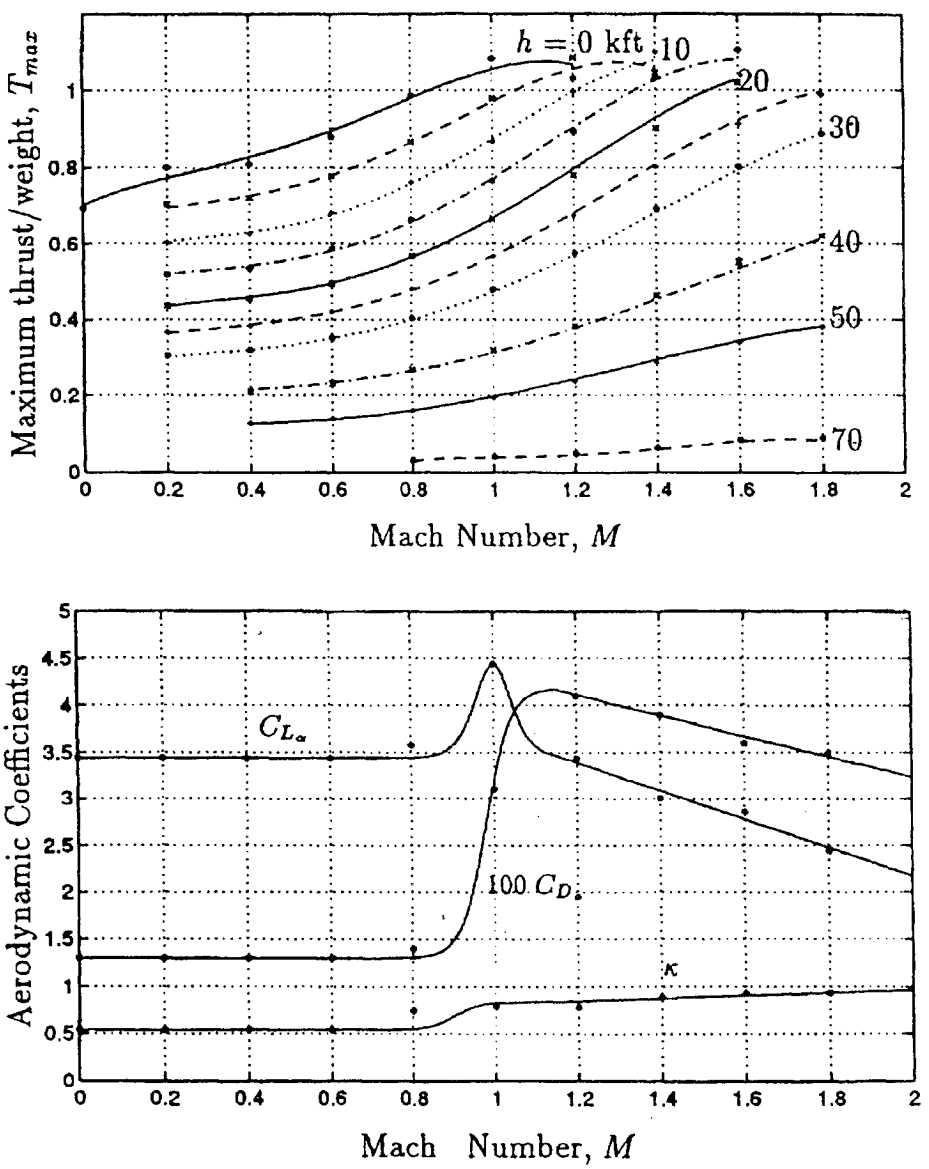

Fig. A1 Aerodynamic and maximum thrust model for F-4H.

satisfying the constraints that deviates as little as possible from the desired outputs can be found using optimal control methods. The inverse solution provides a good initial guess for the iterative algorithm used in the optimal control problem. It also gives preliminary insight into the maneuvers.

The results of minimum radius loop and barrel roll maneuvers show that the maximum thrust/weight ratio and the maximum angle of attack play an important role. There is an optimal $V(0)$, independent of $\chi_c(0)$, for minimum radius maneuvers.

Appendix: F4H Aircraft Model

The aircraft model is taken from Ref. 11 with the following weight (in kilopounds) and wing area (in square feet):

$$W_0 = 35 \tag{A1}$$

$$S = 530 \tag{A2}$$

and

$$C_L = C_{L_\alpha}\alpha \tag{A3}$$

$$C_D = C_{D_0} + \bar{\kappa}C_L^2 \tag{A4}$$

where $\bar{\kappa} = \kappa / C_{L_\alpha}$. The aerodynamic coefficients are approximated as functions of Mach number (see Fig. A1). For $M \leq 1.15$,

$$C_{D_0} = 0.013 + 0.0144\{1 + \tanh[(M - 0.98)/0.06]\} \tag{A5}$$

$$C_{L_\alpha} = 3.44 + \frac{1}{\cosh[(M-1)/0.06]^2} \tag{A6}$$

$$\kappa = 0.54 + 0.15\{1 + \tanh[(M - 0.9)/0.06]\} \tag{A7}$$

For $M > 1.15$,

$$C_{L_\alpha} = 0.013 + 0.0144[1 + \tanh(0.17/0.06)] - 0.011(M - 1.15) \tag{A8}$$

$$C_{D_0} = 3.44 + \frac{1}{[\cosh(0.15/0.06)]^2} - \frac{0.96}{0.63}(M - 1.15) \tag{A9}$$

$$\kappa = 0.54 + 0.15[1 + \tanh(0.25/0.06)] + 0.14(M - 1.15) \tag{A10}$$

and the maximum thrust is approximated as a function of Mach number and altitude

$$T_{\max} = [1 \quad M \quad M^2 \quad M^3 \quad M^4]\, Q\, [1 \quad h \quad h^2 \quad h^3 \quad h^4]^T \tag{A11}$$

where

$$Q = \begin{bmatrix} 30.21 & -0.668 & -6.877 & 1.951 & -0.1512 \\ -33.80 & 3.347 & 18.13 & -5.865 & 0.4757 \\ 100.80 & -77.56 & 5.441 & 2.864 & -0.3355 \\ -78.99 & 101.40 & -30.28 & 3.236 & -0.1089 \\ 18.74 & -31.60 & 12.04 & -1.785 & 0.09417 \end{bmatrix} \tag{A12}$$

References

[1]Kershner, W. K., *The Basic Aerobatic Manual*, Iowa State Univ. Press, Ames, IA, 1990, pp. 24–28, 76–78.

[2]Gunston, B., and Spick, M., *Modern Air Combat*, Crescent Books, New York, 1983, pp. 200–208.

[3]Uehara, S., Stewart, H. J., and Wood, L. J., "Minimum Time Loop Maneuvers of Jet Aircraft," *Journal of Aircraft*, Vol. 15, No. 8, 1995, pp. 449–455.

[4]Shinar, J., Yair, D., and Rotman, Y., "Analysis of Optimal Loop and Split-S by Energy State Modeling," *Israel Journal of Technology*, Vol. 16, 1978, pp. 70–82.

[5]Kato, O., and Sugiura, I., "An Interpretation of Airplane General Motion and Control as Inverse Problem," *Journal of Guidance, Control, and Dynamics*, Vol. 9, No. 2, 1986, pp. 198–204.

[6]Hess, R. A., Gao, C., and Wang, S. H., "Generalized Technique for Inverse Simulation Applied to Aircraft Maneuvers," *Journal of Guidance, Control, and Dynamics*, Vol. 14, No. 5, 1991, pp. 920–926.

[7]Kato, O., "Attitude Projection Method for Analyzing Large Amplitude Airplane Maneuvers," *Journal of Guidance, Control, and Dynamics*, Vol. 13, No. 1, 1990, pp. 22–29.

[8]Sentoh, E., "Comparison of Inverse Control with Optimal Control," Engineering Thesis, Dept. of Aeronautics and Astronautics, Stanford Univ., SUDAAR 590, Stanford, CA, 1990.

[9]Seywald, H., "Trajectory Optimization Based on Differential Inclusion," *Journal of Guidance, Control, and Dynamics*, Vol. 17, No. 3, 1994, pp. 480–487.

[10]Grace, A., "Optimization Toolbox," Math Works Inc., Natick, MA, Dec. 1992.

[11]Bryson, A. E., Desai, M. N., and Foffman, W. C., "Energy-State Approximation in Performance Optimization of Supersonic Aircraft," *Journal of Aircraft*, Vol. 9, No. 2, 1972.